



# HDAC5 Loss Enhances Phospholipid-Derived Arachidonic Acid Generation and Confers Sensitivity to cPLA2 Inhibition in Pancreatic Cancer

Penglin Pan<sup>1,2</sup>, Gengdu Qin<sup>1,2</sup>, Bo Wang<sup>1,2</sup>, Haixin Yu<sup>3</sup>, Jie Chen<sup>4</sup>, Jiaying Liu<sup>4</sup>, Kaijian Bing<sup>5</sup>, Jian Shen<sup>1,2</sup>, Dianyun Ren<sup>1,2</sup>, Yuhan Zhao<sup>1,2</sup>, Wentao Xia<sup>1,2</sup>, Hui Li<sup>6</sup>, Heshui Wu<sup>1,2</sup>, and Yingke Zhou<sup>1,2</sup>

## ABSTRACT

HDAC5 is a class IIa histone deacetylase member that is downregulated in multiple solid tumors, including pancreatic cancer, and loss of HDAC5 is associated with unfavorable prognosis. In this study, assessment of The Cancer Genome Atlas pancreatic adenocarcinoma dataset revealed that expression of HDAC5 correlates negatively with arachidonic acid (AA) metabolism, which has been implicated in inflammatory responses and cancer progression. Nontargeted metabolomics analysis revealed that HDAC5 knockdown resulted in a significant increase in AA and its downstream metabolites, such as eicosanoids and prostaglandins. HDAC5 negatively regulated the expression of the gene encoding calcium-dependent phospholipase A2 (cPLA2), the key enzyme in the production of AA from phospholipids. Mechanistically, HDAC5 repressed cPLA2 expression via deacetylation of GATA1. HDAC5 knockdown in cancer cells enhanced sen-

sitivity to genetic or pharmacologic inhibition of cPLA2 *in vitro* and *in vivo*. Fatty acid supplementation in the diet reversed the sensitivity of HDAC5-deficient tumors to cPLA2 inhibition. These data indicate that HDAC5 loss in pancreatic cancer results in the hyperacetylation of GATA1, enabling the upregulation of cPLA2, which contributes to overproduction of AA. Dietary management plus cPLA2-targeted therapy could serve as a viable strategy for treating HDAC5-deficient pancreatic cancer patients.

**Significance:** The HDAC5-GATA1-cPLA2-AA signaling axis regulates sensitivity to fat restriction plus cPLA2 inhibition in pancreatic ductal adenocarcinoma, proposing dietary management as a feasible strategy for treating a subset of patients with pancreatic cancer.

## Introduction

Histone deacetylases (HDAC) are a group of enzymes that hydrolyze acetylated lysine on histone or non-histone substrates: they are subdivided into four classes (1). Class I HDAC members (including HDAC1, 2, 3, and 8) are commonly deregulated and highly implicated in tumorigenesis and tumor progression (1). Targeted inhibitors for class I HDACs are examined extensively in clinical and preclinical

studies (2). Unlike members of the other HDAC classes, HDAC5, a member of class II HDACs, is typically downregulated or lost in multiple human cancers (3), including pancreatic cancer, and its status correlates markedly with patients' prognoses. However, HDAC5's function has not been investigated fully and remains controversial.

Calcium-dependent phospholipase A2 (cPLA2) encoded by *PLA2G4A* is a key enzyme that promotes the hydrolysis of the acyl-ester bonds of phospholipids on cell membranes, triggering the release of free fatty acids, like arachidonic acid (AA; ref. 4). Freeform AA is further metabolized through the COX, LOX, and CYP pathways, and its metabolites are critically implicated in inflammation and tumorigenesis (5). Inhibitors targeting cPLA2 have seen widespread evaluations in the treatment of cancer, with findings showing that the antitumor effect of inhibiting cPLA2 varies among different cancer types or subtypes (6), indicating that a better understanding of cPLA2 regulation must be sought if cPLA2-targeted therapy is to be applied in cancer treatment.

The GATA-binding protein 1, GATA1, is a master transcription factor (TF) that regulates cell lineage in erythroid and megakaryocytic cells (7). Its mutation or deregulation contributes to inflammatory response, immunity response, and drug resistance in tumors, including pancreatic cancer (8–10). Remarkably, GATA1 is involved in metabolic processes, like lipid metabolism, glycolysis, and oxidative metabolism (11, 12); however, the mechanisms of its involvement remain unknown.

In this study, we identified HDAC5 as an important regulator of AA metabolism in pancreatic cancer. HDAC5's expression correlated negatively with the AA metabolism pathway in patients with pancreatic cancer [The Cancer Genome Atlas (TCGA) pancreatic adenocarcinoma (PAAD) dataset], and HDAC5 mRNA level also had a negative relationship with AA levels in a cohort of pancreatic cancer patient samples. Mechanistically, HDAC5 inhibited AA levels by transcriptionally

<sup>1</sup>Department of Pancreatic Surgery, Union Hospital, Tongji Medical College, Huazhong University of Science and Technology, Wuhan, Hubei, P.R. China.

<sup>2</sup>Sino-German Laboratory of Personalized Medicine for Pancreatic Cancer, Union Hospital, Tongji Medical College, Huazhong University of Science and Technology, Wuhan, P.R. China. <sup>3</sup>Cancer Center, Union Hospital, Tongji Medical College, Huazhong University of Science and Technology, Wuhan, P.R. China.

<sup>4</sup>Department of Pathology, Union Hospital, Tongji Medical College, Huazhong University of Science and Technology, Wuhan, P.R. China. <sup>5</sup>Department of Breast and Thyroid Surgery, Union Hospital, Tongji Medical College, Huazhong University of Science and Technology, Wuhan, P.R. China. <sup>6</sup>Center for Human Genome Research, Key Laboratory of Molecular Biophysics of the Ministry of Education, College of Life Science and Technology, Huazhong University of Science and Technology, Wuhan, P.R. China.

P. Pan, G. Qin, and B. Wang contributed equally to this article.

**Corresponding Authors:** Yingke Zhou, Union Hospital, Tongji Medical College, Huazhong University of Science and Technology, Wuhan 430022, P.R. China. Phone: 8618-1861-28171; E-mail: zykwhuh@hust.edu.cn; Hui Li, huili0930@hust.edu.cn; and Heshui Wu, heshuiwu@hust.edu.cn

Cancer Res 2022;82:4542-54

doi: 10.1158/0008-5472.CAN-21-4362

This open access article is distributed under the Creative Commons Attribution-NonCommercial-NoDerivatives 4.0 International (CC BY-NC-ND 4.0) license.

©2022 The Authors; Published by the American Association for Cancer Research

repressing cPLA2 GATA1-dependently. HDAC5 mediated deacetylation on the C-terminal of GATA1 and decreased the chromatin occupancy of GATA1 on its target gene loci, including *PLA2G4A* (the gene encoding cPLA2). More importantly, we demonstrated that cPLA2 is an effective and promising therapeutic target in HDAC5-deficient pancreatic cancer models *in vivo* and *in vitro*. Furthermore, supplementing a high-fat diet with omega-6 fatty acid reversed sensitivity by rebuilding the production of AA. Conclusively, we have provided a scientific rationale for the combined use of cPLA2 inhibitors and dietary management as a feasible therapeutic strategy for HDAC5 downregulation in patients with pancreatic ductal adenocarcinoma (PDAC).

## Materials and Methods

### Patient materials

All patients were operated on in the Wuhan Union Hospital for pancreatic cancer between 2016 and 2021, and the cancer tissues were collected from the surgeries as diagnostic FFPEs. All the 46 samples used were from pancreaticoduodenectomies or distal pancreatectomies. HDAC5 mRNA expression and arachidonic acid level were analyzed in the patient cohort as described below. Each patient was informed about this research and written informed consent was obtained from them, and the institutional ethical committee has approved the research.

### Cell culture and transfection

All the cell lines in this study were cultured in DMEM (Code No. 11965092, Gibco) containing 10% FBS (Code No. 10099141, Gibco) in a 5% CO<sub>2</sub> environment at 37°C. Lookout *Mycoplasma* PCR Detection Kit (Code No. MP0035, Sigma-Aldrich) was used to regularly examine *Mycoplasma*. All these cell lines were routinely authenticated for purity and being infection free. The plasmids were transfected into cells using Lipofectamine 2000 reagent (Code No. 11668030, Thermo Fisher Scientific), according to the manufacturer's instructions. Lipofectamine 2000 and plasmid were diluted with Opti-MEM (Code No. 11058021, Gibco) separately, then mixed and incubated them at room temperature for 5 minutes. After incubation, the DNA-lipid complex was added to the cells. About 4–8 µg plasmids were used for 1 × 10<sup>6</sup> cells. All the catalog numbers of plasmids are provided in Supplementary Table S1.

### RNAi

Lentivirus-based short hairpin RNA (shRNA) sequencing was provided by Sigma-Aldrich (Code No. TRCN0000004835 for shHDAC5-1, Code No. TRCN0000004836 for shHDAC5-2). The lentiviral packaging vectors psPAX2 and pMD2.G (kindly given by Dr. Haojie Huang, Mayo Clinic) were transfected into 293T cells along with specific shRNA. Replace the culture medium with fresh DMEM with 10% FBS 24 hours after transfection. Viral supernatants were collected 72 hours after transfection. Then the virus containing medium was added to cancer cells with polybrene (12 µg/mL, Code No. C0351, Beyotime Biotechnology). Puromycin (Code No. ST551, Beyotime Biotechnology) was used to select stable transfections at concentration ranges between 3 and 5 µg/mL 48 hours after infection. The sequence information of shRNA is provided in Supplementary Table S2.

### qRT-PCR

Total RNA was isolated from cancer cells using TRIzol reagent (Code No. 15596018, Thermo Fisher Scientific), and then 2 µg RNA was used to perform reverse transcription with a PrimeScript RT reagent Kit (Code No. RR037A, Takara Bio Inc.). The acquired cDNAs

were used for quantitative real-time PCR analysis by using TB Green Fast qPCR Mix PCR kit (Code No. RR430A, Takara Bio Inc.) according to the manufacturer's instruction. The relative fold change was calculated using the 2<sup>-ΔΔC<sub>t</sub></sup> method by normalizing to GAPDH. The specific primers used for qRT-PCR are provided in Supplementary Table S2.

### Coimmunoprecipitation and Western blot analysis

Cells were treated with 1 mL immunoprecipitation (IP) lysis buffer (Code No. P0013, Beyotime Biotechnology) on ice for 30 minutes along with 1 mmol/L phenylmethylsulfonylfluoride (PMSF; Code No. P1046, Beyotime Biotechnology), then cell lysate was centrifuged at 12,000 rpm at 4°C for 15 minutes. Then, the supernatants separately added primary antibody and protein A/G agarose beads (Code No. P2055, Beyotime Biotechnology) and incubated at 4°C overnight. Ice-cold IP lysis buffer (Code No. P0013, Beyotime Biotechnology) was used to wash beads on ice for six times, and the beads were harvested for Western blotting. The protein concentration was determined using a bicinchoninic acid protein assay (Code No. P0012S, Beyotime Biotechnology). Equal amounts of denatured proteins were transferred to polyvinylidene difluoride membranes (Code No. IPVH00005) by SDS-PAGE analysis. The membrane was blocked by 1 × TBST with 5% nonfat milk powder at room temperature for 1 hour. Then specific primary antibodies were added to the membrane for incubating at 4°C overnight. Followed by addition of 1 × TBST (Code No. PPB001, Millipore for TBS and Code No. GC204002, Servicebio for Tween 20) to wash the membrane for three times. Finally, specific secondary antibodies were used to incubate the membrane at room temperature for 2 hours. The samples were detected using a super-sensitive electrochemiluminescence reagent (catalog no. MA0186, Meilunbio). Working dilution of antibodies in this study is provided in Supplementary Table S3.

### RNA sequencing

RNA sequencing was conducted by HaploX. Total RNA samples were prepared by TRIzol reagent (Code No. 15596018, Thermo Fisher Scientific). A total of 1% Agarose gels was used to monitor the degradation and contamination of RNA and the purity of RNA also was checked by NanoPhotometer spectrophotometer (IMPLEN). RNA Nano 6000 Assay Kit of the Bioanalyzer 2100 system (Agilent Technologies) was used to identify RNA integrity. A total of 0.1–1 µg total RNA was used for library construction using NEBNext Ultra mRNA Library Prep Kit for Illumina. As for the quality control of library, Qubit dsDNA HS Assay Kit was used to measure the concentration of library, then D100 Screen Tape was used to examine the distribution of segments in library. KAPA Library Quant Kit universal qPCR Mix (Illumina) was used to measure molarity of library precisely. At last, NovaSeq 6000 and NovaSeq S4 reagent Kit was used for library sequencing.

### Flow cytometric analysis

For flow cytometry analysis of the mouse tissue samples, single-cell suspensions were prepared and stained for flow cytometry with the following antibodies: APC-conjugated CD3 antibody (BioLegend, 100236); FITC-conjugated CD4 antibody (BioLegend, 100510); PerCP-conjugated CD45 antibody (BioLegend, 103130); PE-conjugated CD8 antibody (BioLegend, 100708). After 15 minutes incubation at room temperature, cells were washed three times for 10 minutes each time with PBS, the cells were then resuspended in PBS and analyzed by flow cytometry. Data were analyzed with FlowJo.

### Tissue microarray and IHC

The tissue microarray (TMA) slides were provided by Avilabio (DC-Pan01020). The TMA slides were immunostained with respective specific antibodies (cPLA2 1:50 and HDAC5 1:2,000). The staining intensity was scored in blinded fashion: 1 = weak staining; 2 = medium staining; 3 = strong staining. The positive percentage was defined as follow: 0 = 0%, 1 = 1%–25%, 2 = 26%–50%, 3 = 51%–75%, 4 = above 75%. The staining intensity was calculated by the function: SI = (positive cells% \* the staining intensity). Then, the median value of cPLA2 and HDAC5 scoring in all samples was chosen as the cut-off value. Two independent pathologists who were not aware of the experiments performed the assessment.

### AA quantification by ELISA

The plasmid-transfected cells were cultured in DMEM without AA in a 5% CO<sub>2</sub> environment at 37°C for 24 hours, then the medium was collected and stored at –80°C for further analysis. ELISA kit (Code No. LE-H0939, Lai Er Bio-Tech) was performed according to the manufacturer's protocol. Absorbance values were detected at 450 nm using a full-wavelength microplate reader (Thermo Fisher Scientific). Information of chemicals and kits is provided in Supplementary Table S4.

### Colony formation assay

For the colony formation assay, about 500 cells were seeded into 6-well plates and incubated and cultured in DMEM containing 10% FBS in a 5% CO<sub>2</sub> environment at 37°C for 14 days, they were fixed with methanol and stained with 0.1% crystal violet.

### GST pulldown assay

Cells transfected with GST-tag segments of HDAC5 plasmids were lysed with IP lysis buffer (Code No. P0013, Beyotime Biotechnology) on ice about 0.5 hour, followed by ultrasonication. GST fusion proteins were purified using GST fusion protein purified magnetic beads (Sorlabio Life Science). Then the purified proteins beads were incubated along with cell lysates overnight at 4°C. The beads were washed eight times on ice using ice-cold binding buffer (20 mmol/L Tris, 100 mmol/L NaCl, 1 mmol/L EDTA, 5% Glycerol, 1 mmol/L DTT, 1 mmol/L PMSF, 1 mmol/L Benzamidine) and proteins were eluted on ice using ice-cold IP lysis buffer and analyzed by Western blotting.

### Orthotopic implantation of pancreatic cancer model

In addition, a total of  $5 \times 10^7$  cells were suspended in 10  $\mu$ L volume with PBS and were orthotopically injected into the tail of the pancreas in each mouse from different groups (mice were randomly divided into 12 groups using random digital table). There are 120 mice in total and 10 for each group based on previous report (13). *In vivo* tumor growth was monitored twice per week. Mice were sacrificed 4 weeks after inoculation. The housing conditions were environmental temperatures of 21°C–27°C with 40%–60% humidity and 12-hour light/dark cycle. All animal studies were approved and performed by the animal institute of Tongji Medical College of Huazhong University of Science and Technology and the ethical code is IACUC 2584.

### Nontargeted metabolomic

Analysis was performed using an UHPLC (1290 Infinity LC, Agilent Technologies) coupled to a quadrupole time-of-flight (TOF; AB Sciex TripleTOF 6600) in Shanghai Applied Protein Technology Co., Ltd. For hydrophilic interaction liquid chromatography (HILIC) separation, samples were analyzed using a 2.1 mm  $\times$  100 mm ACQUITY UPLC BEH 1.7  $\mu$ m column (Waters). In both ESI positive and negative

modes, the mobile phase contained A = 25 mmol/L ammonium acetate and 25 mmol/L ammonium hydroxide in water and B = acetonitrile. The gradient was 85% B for 1 minute and was linearly reduced to 65% in 11 minutes, and then was reduced to 40% in 0.1 minute and kept for 4 minutes, and then increased to 85% in 0.1 minute, with a 5-minute reequilibration period employed. For reverse-phase liquid chromatography separation, a 2.1 mm  $\times$  100 mm ACQUITY UPLC HSS T3 1.8  $\mu$ m column (Waters) was used. In ESI positive mode, the mobile phase contained A = water with 0.1% formic acid and B = acetonitrile with 0.1% formic acid; and in ESI negative mode, the mobile phase contained A = 0.5 mmol/L ammonium fluoride in water and B = acetonitrile. The gradient was 1% B for 1.5 minutes and was linearly increased to 99% in 11.5 minutes and kept for 3.5 minutes. Then it was reduced to 1% in 0.1 minute and 3.4 minutes of reequilibration period was employed. The gradients were at a flow rate of 0.3 mL/minute, and the column temperatures were kept constant at 25°C. A 2  $\mu$ L aliquot of each sample was injected. The ESI source conditions were set as follows: Ion Source Gas1 (Gas1) as 60, Ion Source Gas2 (Gas2) as 60, curtain gas (CUR) as 30, source temperature: 600°C, Ion Spray Voltage Floating (ISVF)  $\pm$  5,500 V. In mass spectrometry (MS) only acquisition, the instrument was set to acquire over the m/z range 60–1,000 Da, and the accumulation time for TOF MS scan was set at 0.20 seconds/spectra. In auto MS-MS acquisition, the instrument was set to acquire over the m/z range 25–1,000 Da, and the accumulation time for product ion scan was set at 0.05 seconds/spectra. The product ion scan is acquired using information dependent acquisition with high-sensitivity mode selected. The parameters were set as follows: the collision energy was fixed at 35 V with  $\pm$  15 eV; declustering potential, 60 V (+) and –60 V (–); exclude isotopes within 4 Da, candidate ions to monitor per cycle: 10.

### Chromatin immunoprecipitation sequencing and bioinformatics analyses

Chromatin immunoprecipitation (ChIP) DNA degradation and contamination was monitored on agarose gels. DNA purity was checked using the NanoPhotometer spectrophotometer (IMPLEN). DNA concentration was measured using Qubit DNA Assay Kit in Qubit 3.0 Fluorometer (Life Technologies). Purified DNA was then prepared for ChIP sequencing (ChIP-seq) library generation. The library was constructed by Novogene Corporation. Subsequently, pair-end sequencing of sample was performed on Illumina platform (Illumina). Library quality was assessed on the Agilent Bioanalyzer 2100 system. Raw data (raw reads) of fastq format were firstly processed using fastp (version 0.19.11, Chen and colleagues, 2018) software. In this step, clean data (clean reads) were obtained by removing reads containing adapter, reads containing ploy-N and low quality reads from raw data. At the same time, Q20, Q30, and GC content of the clean data were calculated. All the downstream analyses were based on the clean data with high quality. Reference genome and gene model annotation files were downloaded from genome website directly. Index of the reference genome was built using Burrows-Wheeler Aligner (BWA; v 0.7.12) and clean reads were aligned to the reference genome using BWA (v 0.7.12). The position of peak summit around transcript start sites of genes can predict the interaction sites between protein and gene. ChIPseeker (Yu and colleagues, 2015) was used to retrieve the nearest genes around the peak and annotate genomic region of the peak. Peak-related genes were confirmed by ChIPseeker, and then Gene Ontology (GO) enrichment analysis was performed to identify the function enrichment results. GO enrichment analysis was implemented by the Goseq R package, in which gene length bias was corrected. GO terms with corrected *P* value less

than 0.05 were considered significantly enriched by peak-related genes. Kyoto Encyclopedia of Genes and Genomes (KEGG) is a database resource for understanding high-level functions and utilities of the biological system, such as the cell, the organism and the ecosystem, from molecular-level information, especially large-scale molecular datasets generated by genome sequencing and other high-throughput experimental technologies (<http://www.genome.jp/kegg/>). We used KOBAS software to test the statistical enrichment of peak-related genes in KEGG pathways. Different peak analysis was based on the fold enrichment of peaks of different experiments. A peak was determined as different peak when the OR between two groups was more than 2. Using the same method, genes associated with different peaks were identified and also do GO and KEGG enrichment analysis.

### ChIP and ChIP-qPCR

ChIP assays were performed in pancreatic cancer cells transfected with shHDAC5 and Flag-HDAC5 using the Pierce Magnetic ChIP Kit (Code No. 26157, Thermo Fisher Scientific) according to the manufacturer's instructions. Protein G magnetic beads and specific antibody were used for IP of chromatin, about 5 µg antibodies were used for 25 µg chromatin. In addition, normal rabbit IgG was served as negative control. Finally, PCR Kit (Promega) was performed to purified input and immunoprecipitated DNA. After purification, qPCR was used to check the promoters and enhancers of the DNA samples. The sequences of the primers were provided in Supplementary Table S1. The antibodies used were provided in Supplementary Table S2.

### MTS assay

All tumor cells' proliferation ability was detected by 3-(4,5-dimethylthiazol-2-yl)-5-(3-carboxymethoxyphenyl)-2-(4-sulfophenyl)-2H-tetrazolium (MTS) assay according to the manufacturer's instructions. The absorbance was read at 490 nm by a Biotex Model micro plate reader. Cell viability (%) was calculated using the following formula: Cell viability (%) = (OD sample/OD control) × 100 (3) where OD is the absorbance from the microplate reader.

### Statistical analysis

Statistical computations were performed using SPSS version 22 software (SPSS Inc.). Spearman rank correlation was used to analyze the relationship between two groups. The results are shown as the means ± SD. *P* values under 0.05 were considered as statistically significant for all tests.

### Data availability statement

The data used and/or analyzed during the current study are available from the corresponding author (Heshui Wu, [heshuiwu@hust.edu.cn](mailto:heshuiwu@hust.edu.cn); Yingke Zhou, [zykwhuh@hust.edu.cn](mailto:zykwhuh@hust.edu.cn)) on reasonable request. The ChIP-seq and RNA sequencing (RNA-seq) data have been deposited to the Gene Expression Omnibus database with the accession number GSE185837.

## Results

### HDAC5 loss resulted in enhanced AA metabolism

To elucidate the function of HDAC5 in pancreatic cancer, we analyzed data from TCGA PAAD dataset and found that HDAC5 expression was significantly associated with favorable overall survival and disease-free survival (Supplementary Fig. S1A and S1B). IHC analysis of the samples in the cohort of paired normal and tumor specimens from patients with PDAC revealed considerably

downregulated HDAC5 in PDAC tumor tissues (Supplementary Fig. S1C and S1D).

To uncover the specialized function of HDAC5, we identified differentially expressed genes between low HDAC5-expressing and high HDAC5-expressing patients (Supplementary Fig. S2A). Low HDAC5-expressing patients harbored 2439 upregulated genes (Supplementary Fig. S2B). And, according to gene set enrichment analysis (GSEA) of KEGG pathway, pathways including cell cycle and homologous recombination and AA metabolism were significantly activated (Fig. 1A; Supplementary Fig. S2C and S2D).

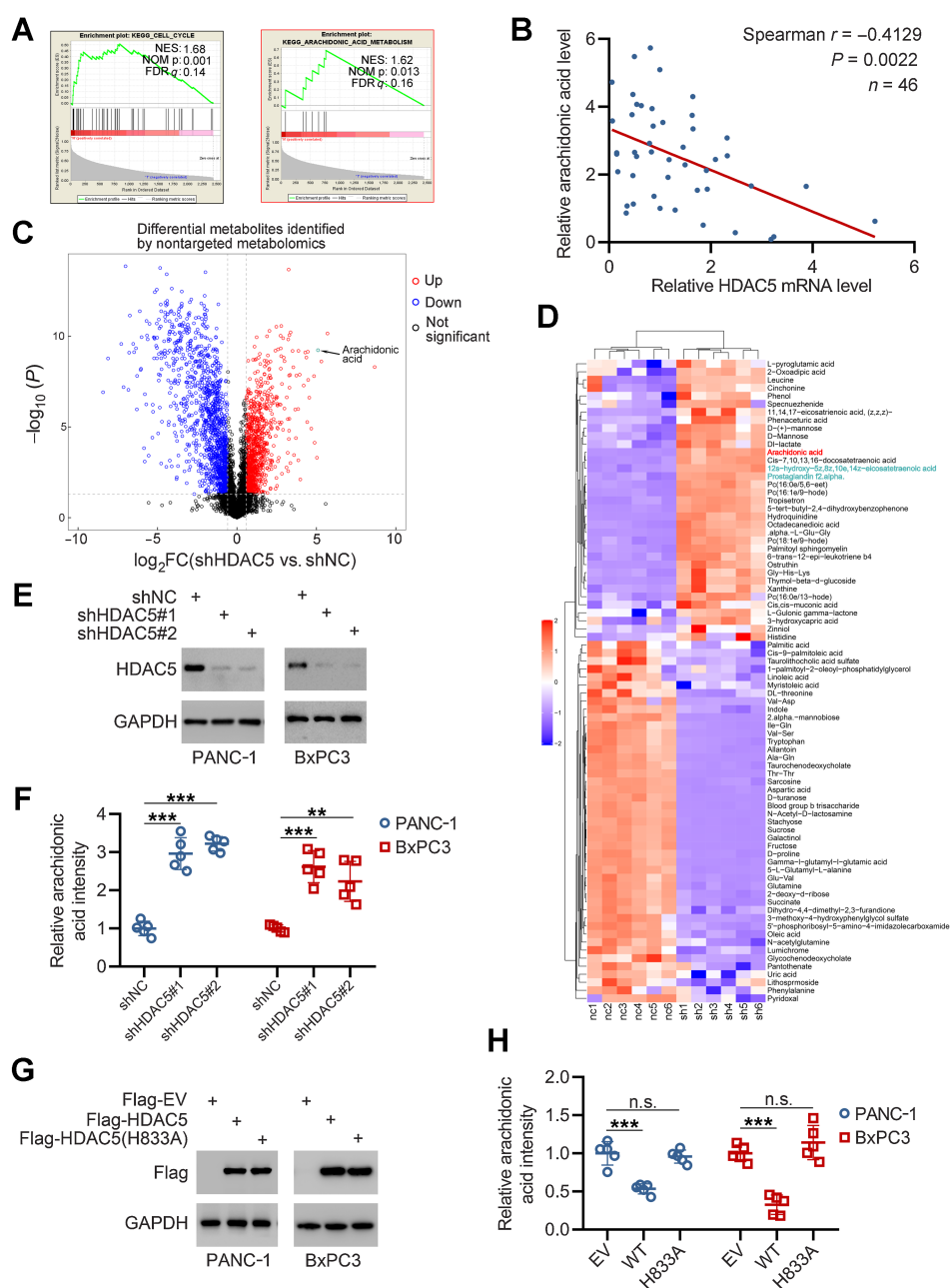
The AA metabolism pathway plays a critical role in proinflammatory responses in cancer (5), with the level of AA and its regulators abnormally elevated in pancreatic cancer via unknown mechanisms (14, 15). To assess HDAC5's impact on AA metabolism, we examined relative HDAC5 mRNA expression and AA levels in the same cohort of pancreatic cancer tissues as shown in Supplementary Fig. S1C. Our results showed that HDAC5 mRNA expression was negatively associated with AA levels (Spearman  $r = -0.4985$ ,  $P = 0.0013$ ; Fig. 1B). More importantly, nontargeted metabolomics revealed that HDAC5 knockdown resulted in a significant elevation in the level of AA and its downstream metabolites, including eicosanoids and prostaglandin (Fig. 1C and D). Knocking down HDAC5 in two pancreatic cancer cell lines using two independent shRNAs resulted in the same outcome, a remarkable rise in AA levels in PANC-1 and BxPC3 cells (Fig. 1E and F; Supplementary Fig. S2E).

Because HDAC5 is a deacetylase that targets histone or non-histone substrates, we sought to know whether HDAC5 requires enzymatic activity to regulate AA levels. To achieve our goal, we constructed a catalytically inactivated mutant [HDAC5(H833A)] as described previously (16). Per our findings, only the ectopic expression of wildtype (WT) HDAC5 repressed AA levels in PANC-1 and BxPC3 cells, with the HDAC5(H833A) mutant expression exhibiting no significant impact on AA levels in these cell lines (Fig. 1G and H). Taken together, our results indicate that HDAC5 inhibits AA levels in pancreatic cancer in a manner dependent on its enzymatic activity.

### HDAC5 inhibits AA production by transcriptionally repressing cPLA2

To determine how HDAC5 represses AA production, we performed RNA-seq analysis in control and HDAC5 knockdown PANC-1 and BxPC3 cells (Supplementary Fig. S3A–S3E). We found that genes encoding key enzymes of the AA metabolism process, including *PLA2G4A* and *ALOX5* were significantly upregulated in HDAC5 knockdown cells (Fig. 2A). *PLA2G4A* encoded an enzyme (cPLA2) responsible for the endogenous release of AA from phospholipids, while *ALOX5* encoded enzymes participating in the metabolism of the downstream metabolites of AA, such as leukotrienes. Therefore, we inferred that HDAC5 inhibited AA levels by repressing cPLA2 expression. We confirmed that HDAC5 knockdown increased cPLA2 protein and cPLA2 mRNA levels (Fig. 2B and C).

IHC analysis of TMAs in a cohort of tumor samples from patients with pancreatic cancer established a negative correlation between HDAC5's expression and cPLA2 protein levels (Spearman  $r = -0.3648$ ,  $P = 0.001$ ,  $n = 78$ ; Fig. 2D and E). Similarly, HDAC5 mRNA levels correlated negatively with *PLA2G4A* mRNA levels in the analyzed data from TCGA PAAD dataset (Spearman  $r = -0.27$ ,  $P = 8.376e-4$ ,  $n = 149$ ; Fig. 2F). More importantly, HDAC5 knockdown failed to trigger an increase in AA levels after cPLA2 knockdown or ASB14780-targeted cPLA2 inhibition (Fig. 2G–I). Our results suggest that HDAC5 repressed AA levels by inhibiting cPLA2 expression (Fig. 2J).

**Figure 1.**

HDAC5 loss resulted in enhanced arachidonic acid metabolism. **A**, GSEA output of the significantly upregulated pathways in HDAC5 loss patients. **B**, Dot plot showing the correlation between HDAC5 mRNA expression and arachidonic acid level in a cohort of pancreatic cancer patients' samples. **C**, Volcano plot showing the metabolites status in HDAC5 knockdown PANC-1 cells compared with control cells via metabolomic analysis. **D**, Heatmap depicting the significantly altered metabolites between HDAC5 knockdown cells and control cells. **E**, Western blot analysis showing the knockdown efficiency of HDAC5 in indicated cell lines. **F**, Relative AA intensity in indicated cell lines. Data are shown as mean  $\pm$  SD;  $n = 5$ . **G** and **H**, Cells were transfected with indicated plasmids for 48 hours and then were harvested for Western blot analysis (**G**) and AA intensity measurement via ELISA assay (**H**). Data are shown as mean  $\pm$  SD;  $n = 5$ . n.s., not significant; \*\*,  $P < 0.01$ ; \*\*\*,  $P < 0.001$ .

### HDAC5 modulates GATA1-dependent cPLA2 expression

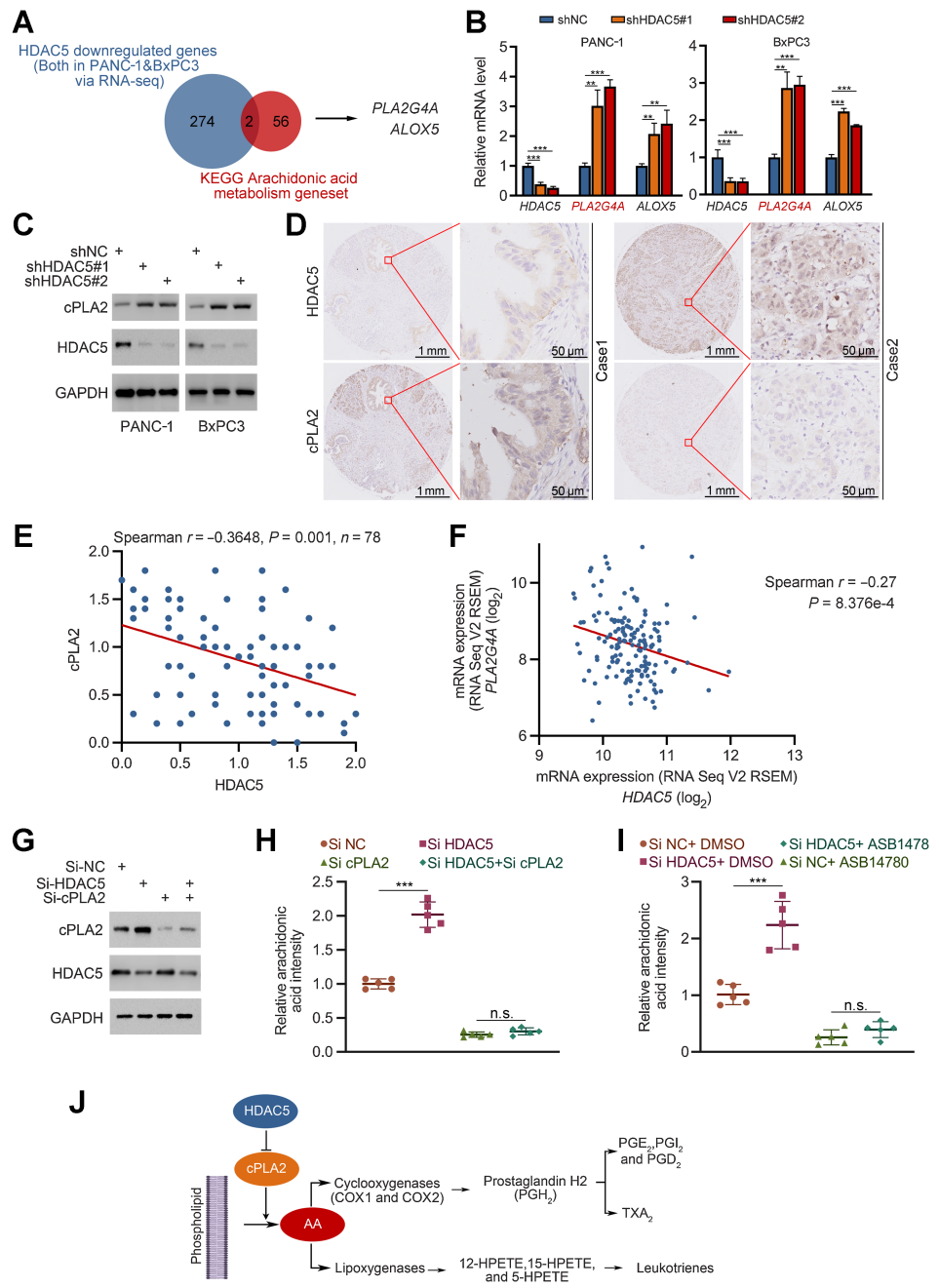
To determine how HDAC5 suppresses cPLA2 expression, we performed ChIP-qPCR analysis to test HDAC5's ability to regulate histone acetylation in the gene loci of *PLA2G4A* (Fig. 3A and B; ref. 3). Consistent with our previous observation, the knockdown of HDAC5 significantly increased the overall level of histone modifications that activate transcription, such as H3ac and H3K27ac (Supplementary Fig. S4A). However, knockdown HDAC5 failed to alter H3ac, H3K27ac or H4ac levels on the gene loci of *PLA2G4A* (Fig. 3B; Supplementary Fig. S4B).

Because HDAC5 reportedly interacts with some non-histone TFs and regulates their transcriptional activity (17, 18), we assessed HDAC5's ability to regulate cPLA2 expression via similar mechan-

isms. We identified 33 TFs of cPLA2 by conducting a TF-binding motif analysis of the promoter region of *PLA2G4A* (Fig. 3C). Our results showed that only two proteins (GATA1 and HNF1A) of all the identified TFs were apparent in the MS-based HDAC5 interactome (Fig. 3C). Astonishingly, knocking down HDAC5 did not alter *PLA2G4A* mRNA levels after GATA1 knockdown but did so post-HNF1A silencing (Fig. 3D). Similarly, the ectopic overexpression of HDAC5 only minimally impacted cPLA2 expression post-GATA1 knockdown (Fig. 3E). We further verified this phenomenon using ChIP-qPCR and found that the binding of GATA1 to the promoter region of *PLA2G4A* was massively amplified post-HDAC5 knockdown (Fig. 3F). More importantly, the HDAC5 loss-induced increase in AA level was almost entirely diminished by GATA1 silencing (Fig. 3G

**Figure 2.**

HDAC5 inhibits AA production via transcriptionally repressing cPLA2. **A**, Venn diagram shows the result of analysis of RNA-seq data in PANC-1 and BxPC3 cells, indicating the AA metabolism genes that were significantly repressed by HDAC5. **B** and **C**, PANC-1 and BxPC3 cells were infected with indicated lentivirus for 48 hours; after puromycin selection for 48 hours, cells were harvested for qRT-PCR analysis (**B**) and Western blot analysis (**C**). Data are shown as mean  $\pm$  SD;  $n = 3$ . **D** and **E**, Images of IHC analysis for HDAC5 and cPLA2 on TMA containing a cohort of pancreatic cancer samples ( $n = 78$ ; **D**) and the correlation analysis of IHC staining index of HDAC5 and cPLA2 (**E**). **F**, Correlation analysis of the mRNA level of *HDAC5* and *PLA2G4A* in TCGA PAAD dataset. **G** and **H**, PANC-1 cells were transfected with indicated plasmids for 48 hours, and then were harvested for Western blot analysis (**G**) and AA intensity measurement (**H**). Data are shown as mean  $\pm$  SD;  $n = 5$ . **I**, Cells were transfected with indicated plasmids for 48 hours and then were treated with indicated reagent for 24 hours, and were harvested for AA intensity measurement. Data are shown as mean  $\pm$  SD;  $n = 5$ . **J**, Model depicting the mechanism that HDAC5 inhibits phospholipid-derived arachidonic acid via the repression of cPLA2, the key enzyme in this process. n.s., not significant; \*\*,  $P < 0.01$ ; \*\*\*,  $P < 0.001$ .



and **H**). In addition, HDAC5 overexpression failed to further repress AA levels after GATA1 knockdown (**Fig. 3I** and **J**). Our findings suggest that HDAC5 represses cPLA2 expression and AA generation GATA1-dependently (**Fig. 3K**).

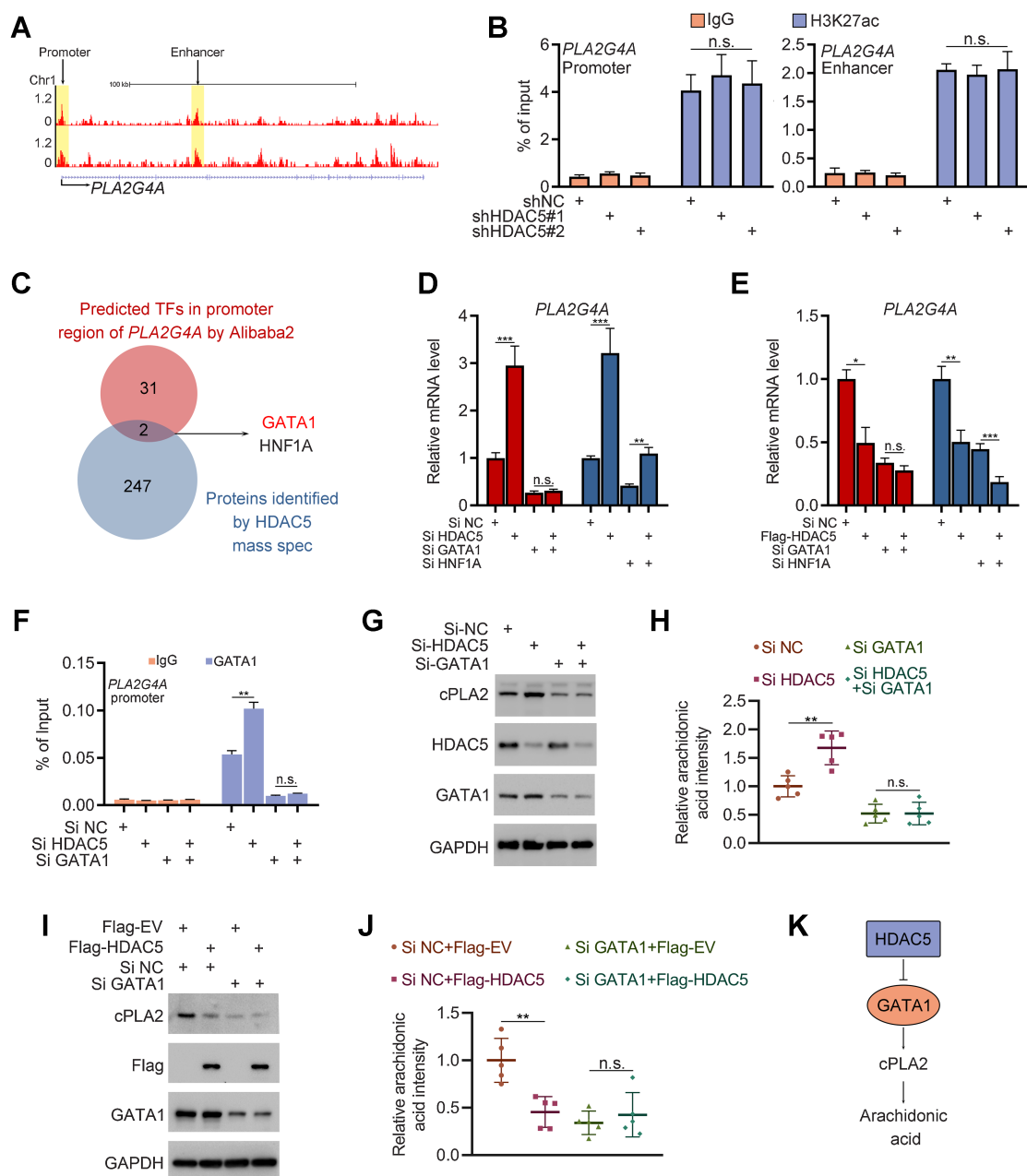
**HDAC5 represses GATA1 chromatin occupancy via GATA1 deacetylation**

HDAC5 regulates AA metabolism via the GATA1-cPLA2 axis (**Figs. 2** and **3**), and its ability to disrupt AA generation relies on its enzyme activity (**Fig. 1G** and **H**). We sought to determine whether HDAC5 regulates GATA1’s transcriptional activity via GATA1 deacetylation.

The mass spectrometry analysis led to the identification of GATA1 as a HDAC5 binding partner (Supplementary Table.S5),

which was furthermore confirmed by endogenous reciprocal co-immunoprecipitation (co-IP; **Fig. 4A**), and we further established that the DAC domain of HDAC5 and the C terminal of GATA1 account for the HDAC5-GATA1 interaction (Supplementary Fig. S5A–S5D). More importantly, as expected, HDAC5 knockdown significantly increased the acetylated lysine levels of the GATA1 protein (**Fig. 4B**) and GATA1 enrichment in the PLA2G4A promoter region (**Fig. 4C**). Also, the overexpression of the WT HDAC5, but not the enzymatic inactivated mutant, HDAC5(H833A), repressed the lysine acetylation of GATA1 and GATA1’s binding to the promoter region of PLA2G4A (**Fig. 4D** and **E**).

To further assess the impact of HDAC5 loss on the genomic distribution of GATA1, we performed GATA1 ChIP-seq in control

**Figure 3.**

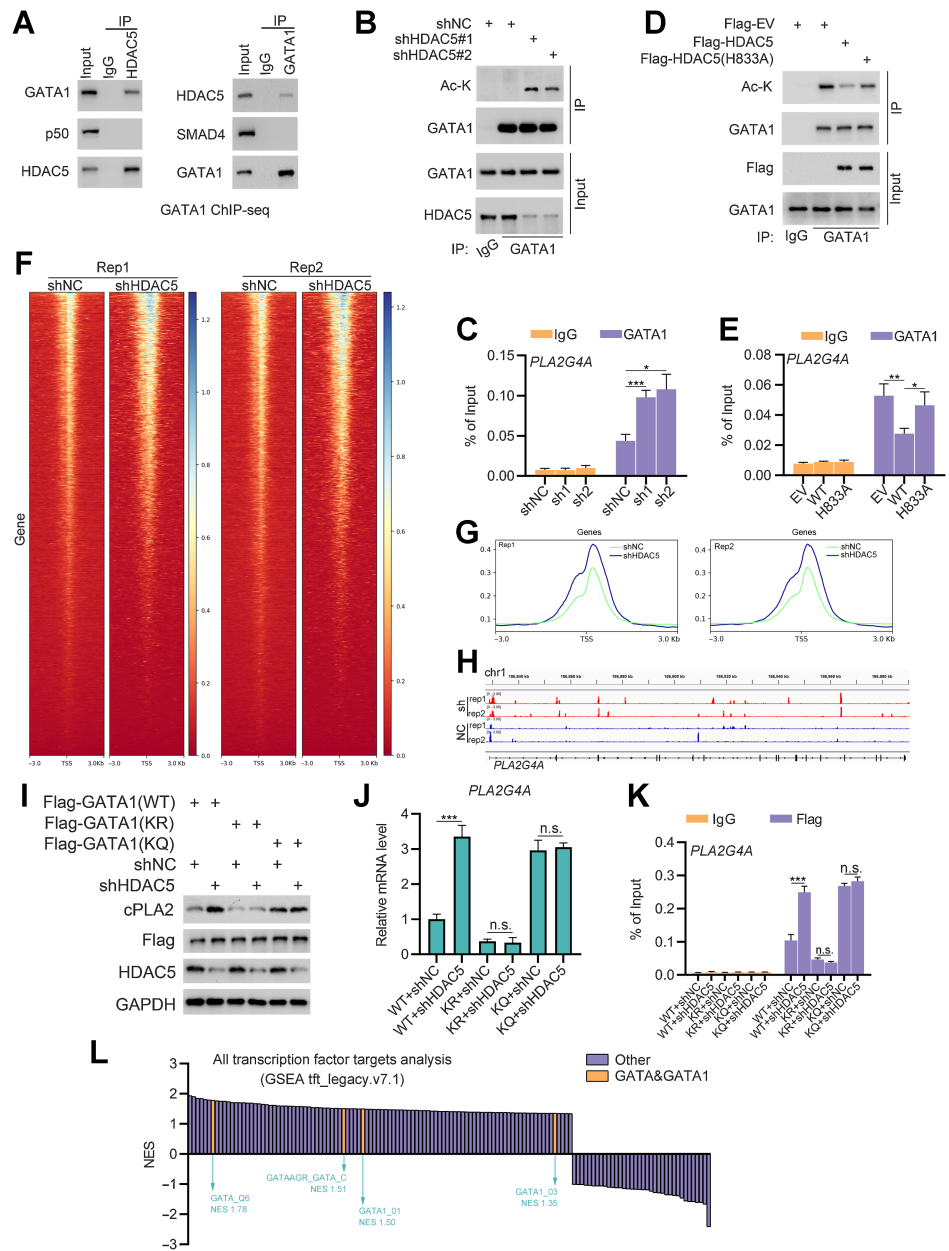
HDAC5 modulates GATA1-dependent cPLA2 expression. **A**, UCSC Genome Browser screenshot of H3K27ac ChIP-seq tracks at the gene loci of *PLA2G4A*. **B**, PANC-1 cells were infected with indicated lentivirus for 48 hours. After a 48 hour puromycin selection, cells were harvested for ChIP-qPCR analysis. Data are shown as mean  $\pm$  SD,  $n = 3$ . **C**, Venn diagram showing the predicted HDAC5-regulated transcription factors of *PLA2G4A*. **D** and **E**, PANC-1 cells were transfected with indicated plasmids for 48 hours and then were harvested for qRT-PCR analysis. Data are shown as mean  $\pm$  SD;  $n = 3$ . **F-H**, PANC-1 cells were transfected with indicated plasmids for 48 hours and then were harvested for ChIP-qPCR analysis (**F**; data are shown as mean  $\pm$  SD;  $n = 3$ ), Western blot analysis (**G**; data are shown as mean  $\pm$  SD;  $n = 5$ ), and AA intensity measurement (**H**; data are shown as mean  $\pm$  SD;  $n = 5$ ). **I** and **J**, PANC-1 cells were transfected with indicated plasmids for 48 hours, and then were harvested for Western blot analysis (**I**) and AA intensity measurement (**J**). Data are shown as mean  $\pm$  SD;  $n = 5$ . **K**, Model depicting the mechanism that HDAC5 represses cPLA2 expression and AA production in a GATA1-dependent manner. n.s., not significant; \*,  $P < 0.05$ ; \*\*,  $P < 0.01$ ; \*\*\*,  $P < 0.001$ .

and HDAC5 knockdown PANC-1 cells (Fig. 4F and G). We found that HDAC5 knockdown resulted in a prominent increase in global GATA1 chromatin binding (Fig. 4F and G). And consistently, the GATA1 binding at the locus of *PLA2G4A* was significantly increased after the knockdown of HDAC5 in ChIP-seq (Fig. 4H).

Reports show that acetylated lysine residues (<sup>310</sup>SGKGGKKRGS<sup>319</sup>) in the GATA1 C-terminal are essential for its chromatin occupancy (19). Therefore, we examined HDAC5's propensity to converge on these residues to regulate the chromatin occupancy of GATA1. To do this, we generated an acetylation-resistant construct by substituting

**Figure 4.**

HDAC5 represses GATA1 chromatin occupancy via GATA1 deacetylation. **A**, PANC-1 cells were harvested for endogenous reciprocal co-IP of HDAC5 and GATA1. **B**, PANC-1 cells were infected with indicated lentivirus for 48 hours. After a 48-hour puromycin selection, cells were harvested for co-IP analysis. **C**, PANC-1 cells were infected with lentivirus-expressing shControl (shNC) or HDAC5-specific shRNAs (sh1 and sh2) for 48 hours; after 48 hours puromycin selection, cells were harvested for ChIP-qPCR analysis. Data are shown as mean  $\pm$  SD;  $n = 3$ . **D**, PANC-1 cells were transfected with indicated plasmids for 48 hours and then were harvested for co-IP assay. **E**, PANC-1 cells were transfected with plasmids containing empty control (EV), WT HDAC5 (WT), and HDAC5 H833A mutant (H833A) for 48 hours, and then were harvested for ChIP-qPCR analysis. Data are shown as mean  $\pm$  SD;  $n = 3$ . **F**, The heatmap view for GATA1 ChIP-seq signal intensity in control PANC-1 cells and HDAC5 knocked down PANC-1 cells. **G**, The mean of GATA1 ChIP-seq signals at its binding sites in indicated groups. **H**, The GATA1 ChIP-seq tracks at the locus of *PLA2G4A* in indicated groups. **I-K**, PANC-1 cells were infected with lentivirus expressing indicated shRNAs for 48 hours and received a puromycin selection for 48 hours. Then cells were transfected with plasmids containing WT GATA1 (WT), GATA1 KR mutant (KR), and GATA1 KQ mutant (KQ) for another 48 hours and were harvested for Western blot analysis (**I**), qRT-PCR analysis (**J**), and ChIP-qPCR analysis (**K**). Data are shown as mean  $\pm$  SD;  $n = 3$ . **L**, Column plot of normalized enriched score (NES) of pathways significantly altered in GSEA of the RNA-seq data of HDAC5 knockdown cells. n.s., not significant; \*,  $P < 0.05$ ; \*\*,  $P < 0.01$ ; \*\*\*,  $P < 0.001$ .



lysine residues with arginine (KR) and an acetylation-mimicking construct by mutating lysine residues into glutamine (KQ; Supplementary Fig. S5E). Per co-IP, manipulating HDAC5 did not affect the levels of the acetylated lysine residues of the GATA1 KR mutant (Supplementary Fig. S5F). However, as expected, KR mutation severely decreased GATA1 enrichment at the promoter region of *PLA2G4A* (Supplementary Fig. S5G), and knocking down HDAC5 increased the enrichment of the WT GATA1, but not that of the KR mutant, at the gene loci of *PLA2G4A* (Supplementary Fig. S5G). Furthermore, Western blot, qRT-PCR, and ChIP-qPCR analyses revealed that the GATA1 KQ mutant steadily promoted the expression of cPLA2 regardless of the status of HDAC5 (Fig. 4I-K). In addition, we performed all TF targets analysis for the downregulated HDAC5 genes identified by RNA-seq using GSEA (tft\_legacy.v.7.1) and found that either one of

GATA1 or GATA was identifiable as one of the most significantly suppressed TFs by HDAC5 (Fig. 4L). Taken together, these results indicate that HDAC5 represses GATA1 chromatin occupancy via GATA1 deacetylation.

As HDAC5 was thought to have a very limited catalytic activity (20), and tend to work as scaffold for other HDAC members such as class I HDACs to complete the process of deacetylation (21). We sought to determine whether any class I HDAC members is responsible for HDAC5-mediated GATA1 deacetylation. However, co-IP indicated that knockdown of any one of HDAC1, 2, or 3 had an insignificant effect on GATA1's acetylation (Supplementary Fig. S6A). While the treatment of HDAC I selectively inhibitor, CHR-3996, significantly elevated the acetylation level of GATA1 as the HDAC5 knockdown did (Supplementary Fig. S6B). More importantly, CHR-3996 fail to further

increase GATA1 acetylation when HDAC5 is knocked down (Supplementary Fig. S6B). And co-IP analysis of endogenous HDAC5 in PANC-1 cells also indicated the valid binding status of HDAC5 and the members of class I HDACs (Supplementary Fig. S6C). Thus, our data infer that HDAC5 might work with class I HDACs to complete the process of GATA1 deacetylation.

**HDAC5 loss in pancreatic cancer confers sensitivity to cPLA2-targeted inhibition**

If abnormally elevated AA levels in non-HDAC5-expressing pancreatic cancer contribute to tumorigenicity, targeting cPLA2 could be a promising therapeutic strategy. Here, HDAC5 knockdown sensitized pancreatic cancer cells to treatment with the cPLA2 inhibitor, ASB14780 (Fig. 5A). Cell culture under exogenous fatty acid-free

conditions, which blocked other compensatory mechanism-derived AAs, amplified this phenomenon (Fig. 5B). Furthermore, ASB14780 treatment considerably inhibited the clonogenicity of HDAC5 knockdown cells, while rescue experiment with the reexpression of HDAC5 abolished this sensitivity (Fig. 5C and D; Supplementary Fig. S7A and S7B). However, exogenous supplementation with AA almost entirely diminished the inhibitory effect of ASB14780 on the viability and clonogenicity of pancreatic cancer cells (Fig. 5B-D; Supplementary Fig. S5A and S5B), indicating that ASB14780's inhibitory effect on non-HDAC5-expressing cells is contingent on the suppression of lipid-derived AA production.

To further confirm the importance of AA to tumor progression after HDAC5 loss, we genetically inhibited cPLA2 in pancreatic cancer patient-derived cells (PDC). Genetically silencing cPLA2 suppressed

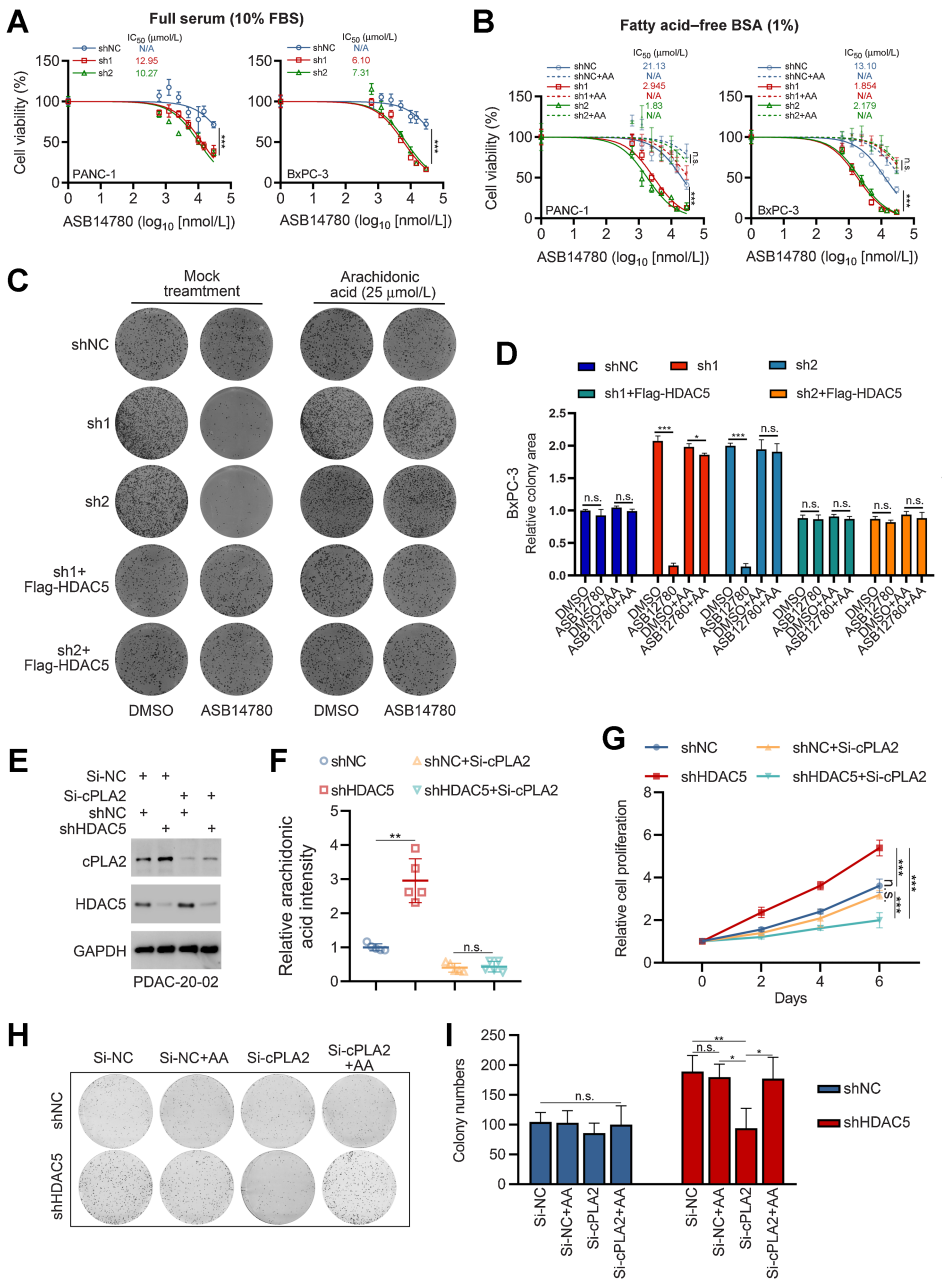


**Figure 5.** HDAC5 loss in pancreatic cancer confers sensitivity to cPLA2-targeted inhibition. **A**, PANC-1 and BxPC3 cells were infected with lentivirus-expressing control (shNC) or HDAC5-specific shRNAs (sh1 and sh2) for 48 hours. After puromycin selection for 48 hours, cells were treated with different doses of ASB14780 for 48 hours and cell viability was measured by MTS assay. **B-D**, After the infection of indicated lentivirus and puromycin selection, PANC-1 and BxPC3 cells were cultured in medium containing 1% fatty acid-free BSA and were treated with different doses of ASB14780 under the condition with or without arachidonic acid (25 μmol/L) for 48 hours. Cell viability was measured by MTS assay (**B**) and the clonogenicity was measured 10 days after plate operation (**C** and **D**). **E-G**, Patient-derived cancer cells were infected with indicated shRNA or siRNA, 48 hours after infection, cells were harvested for Western blot analysis (**E**), arachidonic acid measurement by ELISA (**F**), and cell proliferation assessment by MTS assay (**G**). **H** and **I**, PDCs were infected with indicated shRNA or siRNA, and the clonogenicity of cells was measured 10 days after plate operation. n.s., not significant; \*, *P* < 0.05; \*\*, *P* < 0.01; \*\*\*, *P* < 0.001.

the HDAC5 loss-induced rise in AA levels (Fig. 5E and F) and drastically hindered the proliferation rate and clonogenicity of PDCs, which was, in turn, restored by AA supplementation (Fig. 5G–I). And we also got consistent data by genetically manipulate cPLA2 in HDAC5 loss PANC-1 and BxPC3 cells (Supplementary Fig. S7C–S7H). These data suggest that HDAC5 loss in pancreatic cancers confers sensitivity to cPLA2-targeted inhibition.

COX2, one of the key enzymes for the metabolism of AA, was also thought to be a therapeutic target in certain cancers (5). We were interested whether HDAC5 loss pancreatic cancer models were sensitive to COX2 inhibition. As expected, the knockdown of COX2 did not alter the regulation of HDAC5 on AA (Supplementary Fig. S8A and S8B). And COX2 knockdown only exhibited moderate inhibitory

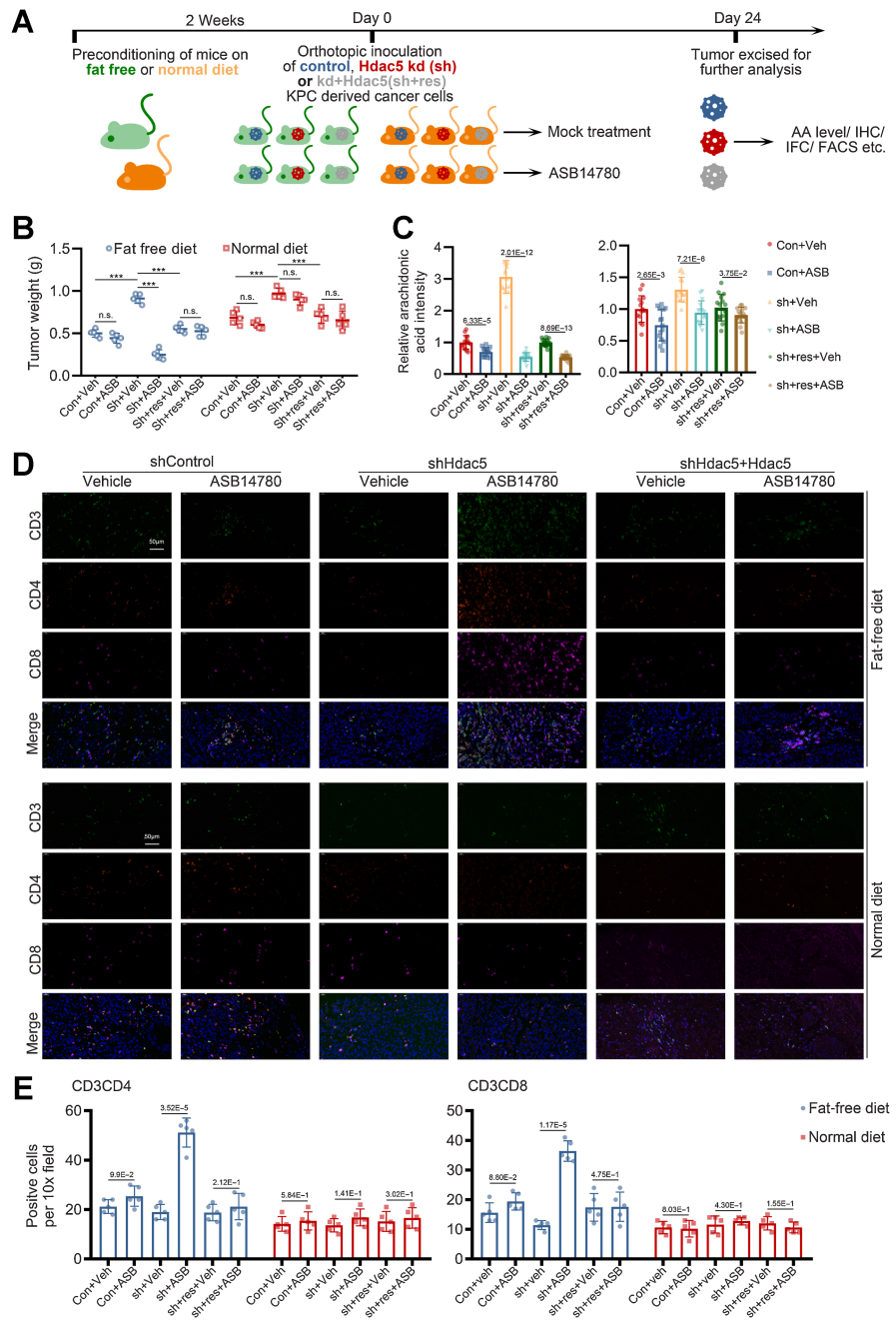
effect on the growth of HDAC5 loss BxPC3 cells. It has no significant effect in PANC-1 cells regardless of the expression of HDAC5 (Supplementary Fig. S8C and S8D).

**cPLA2 inhibition and diet restriction reduce HDAC5 loss-induced tumorigenicity and rebuild tumor immune microenvironment in pancreatic cancer**

Because cPLA2 inhibition and fat-free conditions selectively reduced the tumorigenicity of non-HDAC5-expressing cancer cells, we evaluated dietary fat content’s ability to affect this response *in vivo*. To do so, we generated control, Hdac5 knockdown and Hdac5 reexpressed orthotopic tumor models using KPC (*Kras*<sup>G12D/+</sup>; *LSLTrp53*<sup>R172H/+</sup>; *Pdx-1-Cre*) mouse-derived pancreatic cancer cells.

**Figure 6.**

cPLA2 inhibition and diet restriction reduce HDAC5 loss-induced tumorigenicity and rebuild tumor immune microenvironment in pancreatic cancer. **A**, Diagram depicting the major steps of mouse work. **B–E**, KPC mouse-derived pancreatic cancer cells were injected orthotopically in the pancreas. The tumors were excised 24 days after injection for weighing (B), arachidonic acid intensity measurement (C), immunofluorescence staining analysis (D), and quantification (E). n.s., not significant; \*\*\*, *P* < 0.001.



We treated tumor-bearing mice with a mock treatment or ASB14780, combining the treatment modalities with an isodynamic fat-free diet or a normal fat-containing diet (Fig. 6A). As expected, dietary restriction resulted in a moderate reduction in tumor weight (Fig. 6B; Supplementary Fig. S9A). And, consistent with our earlier observation, Hdac5 knockdown caused a significant increase in tumor weight (Fig. 6B; Supplementary Fig. S9A). Similar to the pharmacologic and genetic inhibition of cPLA2 *in vitro*, treatment with ASB14780 only markedly reduced tumor weight in the Hdac5 knockdown allografts in mice undergoing fat-free rearing; mice raised with the “AA-rich” fat-containing diet displayed a contradictory outcome (Fig. 6B; Supplementary Fig. S9A). ELISA analyses of resected tumors revealed that combining ASB14780 treatment with the fat-free diet completely eradicated Hdac5 loss-induced AA level increase, while dietary supplementation with fatty acids almost entirely abolished the effect (Fig. 6C).

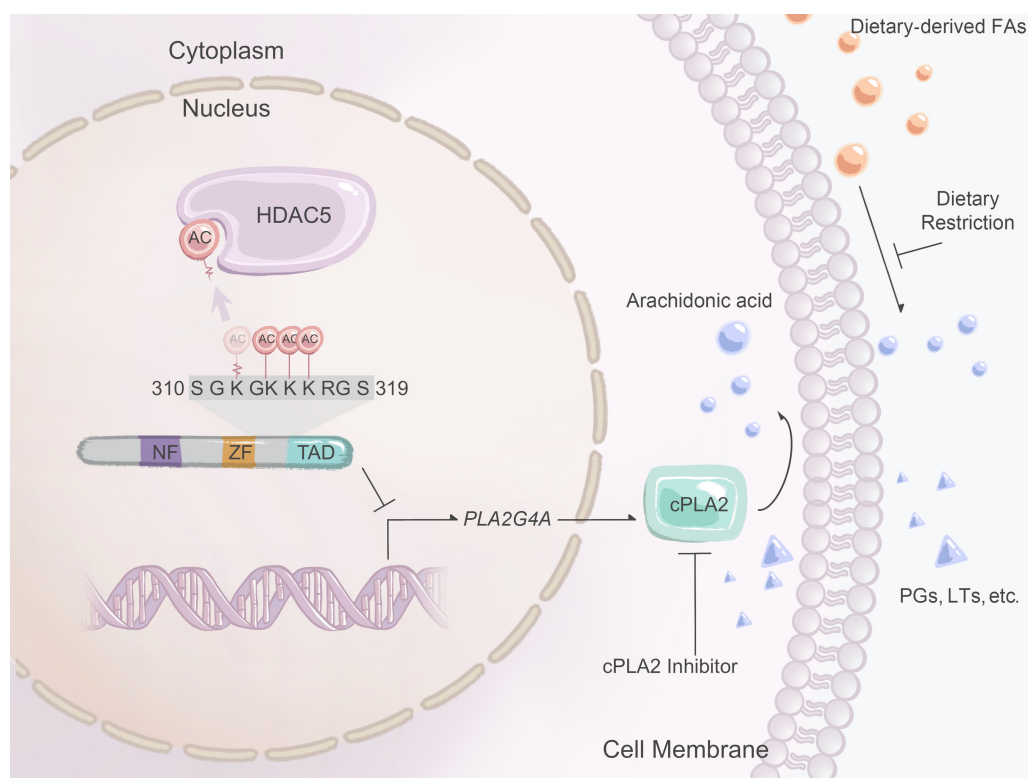
AA and its downstream metabolites, such as prostaglandins, are highly involved in the metabolic remodeling of tumor immunologic microenvironments and contribute to immune evasion and tumor progression (22–24). Therefore, we investigated whether Hdac5 loss-induced AA level increase and cPLA2 inhibition could affect the tumor immune microenvironment. Tumor tissue immunofluorescence showed that Hdac5 loss resulted in a moderate decline in tumor-infiltrating lymphocytes (TIL). TILs, however, increased considerably in the ASB14780 and fat free diet-treated Hdac5 loss allografts (Fig. 6D and E; Supplementary Fig. S9B), but supplementation with the fat-containing diet, regardless of the presence or not of the cPLA2 inhibitor, suppressed this upsurge (Fig. 6D and E; Supplementary

Fig. S9B). We further confirmed this phenomenon by conducting a FACS analysis of tumor samples (Supplementary Fig. S9C). Our findings indicate that HDAC5 loss-induced AA level rise repressed pancreatic cancer tumor immunogenicity, whereas combining cPLA2 inhibition with dietary fat restriction restored tumor immunity by manipulating the AA metabolism.

## Discussion

The interplay between genotype and specific metabolic subtype plays a novel role in the development and progression of pancreatic cancer (25). A thorough investigation of the process enables a better understanding of the pathogenesis and effective therapeutic strategies for the treatment of the dismal disease. In this study, we identified HDAC5 as an important repressor of phospholipid-derived AA, showed that HDAC5 loss in pancreatic cancer induces the overproduction of AA and its metabolites via the overactivated GATA1-cPLA2 axis, linked the poor genotype and HDAC5 loss to a deregulated AA metabolism, and established a new mechanism of HDAC5's regulation of AA production and cancer progression.

Importantly, we also determined the unrevealed transcription suppressor role of HDAC5 via GATA1 deacetylation. HDAC5's role differs in various cancer types (26, 27). Analyses of data from TCGA database indicate that HDAC5 expression is downregulated in most solid tumors (3) and HDAC5 is deleted at the genomic level in multiple cancer types, including pancreatic cancer (28, 29). The prognoses of patients in pan-cancer analyses also suggest that low HDAC5 expression is significantly associated with poor prognosis (29). In



**Figure 7.**

HDAC5 loss in pancreatic cancer induces enhanced phospholipid-derived arachidonic acid via overactivated GATA1-cPLA2 axis. Deficient HDAC5 induces enhanced phospholipid-derived arachidonic acid via deacetylating GATA1 and repressing cPLA2.

addition to the classic corepressor function in the process of chromatin modification regulation (30), HDAC5 regulates gene expression via the deacetylation of many non-histone TFs (16–18). In our current study, we identified GATA1 as a substrate of HDAC5. HDAC5 mediated deacetylation on lysine residues in the C-terminal of the zinc finger region of GATA1 to repress the chromatin occupancy of GATA1 and inhibit GATA1-dependent transcriptional activation. HDAC5 is known as an enzyme-inactivated HDAC member owing to the amino acid exchange in the catalytic center (20). However, it may act as a reader to recognize acetylated lysine residues and recruit other enzymatically active regulators, such as class I HDACs (HDAC1, 2, and 3) to complete the whole process (21). We demonstrated that GATA1's acetylation and chromatin occupancy can be significantly altered by manipulating HDAC5 alone. And HDAC5 might work with multiple class I HDACs or other proteins with deacetylase activity to complete the process of deacetylation; however, this inference warrants further scrutiny. Nevertheless, we identified HDAC5 as an important regulator in the process of GATA1 deacetylation.

GATA1 is a master regulator that controls erythroid and megakaryocyte commitment and differentiation (31). Its dysfunction is intimately linked to leukemogenesis in human Down syndrome cases and mice (7). It is also alleged to be activated and implicated in tumorigenesis and antiapoptosis in pancreatic cancer (9, 32). One proteomic study on kidney fibroblasts established a correlation between GATA1 and fatty acid metabolism; however, the mechanism remains unknown (11). Here, we identified GATA1 as a crucial transcriptional regulator of *PLA2G4A*, the gene that encodes cPLA2, the key enzyme in the conversion of phospholipids to AA (33).

Acetylation is an important posttranslational modification of GATA1 that regulates its transcriptional activity (34). The histone acetyltransferase CREB-binding protein and p300 (CBP/p300) were the first described regulators to promote GATA1 DNA binding or chromatin occupancy via acetylation of lysine residues near the finger domain of GATA1 and further facilitate the recruitment of bromodomain proteins to the chromatin (19, 35, 36). In this study, we found that HDAC5 performed a contrasting role to CBP/p300 in the regulation of GATA1's activity by converging on GATA1 lysine acetylation.

Regulators of the AA metabolism pathway, including phospholipases, lipoxygenases, and cyclooxygenases, are abnormally activated in pancreatic cancer; however, the mechanisms of these actions remain unknown (14, 15). Our current research provided a plausible explanation, one that indicates that HDAC5 loss in pancreatic cancer results in an overactivated GATA1-cPLA2 axis. Of note, our results suggest that HDAC5 loss could also promote the downstream metabolism of

AA, as genes, like *ALOX5*, was also increased significantly upon knocking down HDAC5 (Fig. 3B). However, we also noticed that part of the HDAC5-high patients in TCGA dataset also has a relatively high AA pathway activity (Supplementary Fig. S2D), indicating there might exist unrevealed mechanism that neutralized the effect of HDAC5. And all these findings point to the existence of multiple layers and complexity of this process.

Conclusively, we have established that HDAC5 represses AA overproduction via GATA1 deacetylation and cPLA2 inhibition and shown that cPLA2 inhibition plus dietary fat restriction effectively suppresses HDAC5 loss-induced tumorigenesis and rebuilds the tumor immune microenvironment. Our findings that HDAC5 loss triggers the overactivation of the GATA1-cPLA2 axis, the overproduction of AA, and susceptibility to cPLA2 inhibition plus fat restriction provide an ingenious therapeutic strategy for the treatment of patients with non-HDAC5-expressing pancreatic cancer and highlights the importance of dietary management in the treatment of pancreatic cancer (Fig. 7).

### Authors' Disclosures

No disclosures were reported.

### Authors' Contributions

**P. Pan:** Conceptualization, data curation. **G. Qin:** Data curation, formal analysis. **B. Wang:** Software, formal analysis. **H. Yu:** Software. **J. Chen:** Software, supervision. **J. Liu:** Supervision, investigation, methodology. **K. Bing:** Investigation, visualization, methodology. **J. Shen:** Visualization, project administration. **D. Ren:** Supervision, project administration. **Y. Zhao:** Supervision, validation. **W. Xia:** Validation, investigation. **H. Li:** Conceptualization, investigation. **H. Wu:** Funding acquisition. **Y. Zhou:** Conceptualization.

### Acknowledgments

This study was supported by the Chinese National Natural Science Foundation Grant No. 81872116 (H. Li), 82073178 (H. Wu), and 82102794 (Y. Zhou).

The publication costs of this article were defrayed in part by the payment of publication fees. Therefore, and solely to indicate this fact, this article is hereby marked "advertisement" in accordance with 18 USC section 1734.

### Note

Supplementary data for this article are available at Cancer Research Online (<http://cancerres.aacrjournals.org/>).

Received December 20, 2021; revised July 13, 2022; accepted September 8, 2022; published first September 14, 2022.

### References

- Marks P, Rifkin RA, Richon VM, Breslow R, Miller T, Kelly WK. Histone deacetylases and cancer: causes and therapies. *Nat Rev Cancer* 2001;1:194–202.
- Romero D. HDAC inhibitors tested in phase III trial. *Nat Rev Clin Oncol* 2019;16:465.
- Zhou Y, Jin X, Ma J, Ding D, Huang Z, Sheng H, et al. HDAC5 loss impairs RB repression of pro-oncogenic genes and confers CDK4/6 inhibitor resistance in cancer. *Cancer Res* 2021;81:1486–99.
- Wang B, Wu L, Chen J, Dong L, Chen C, Wen Z, et al. Metabolism pathways of arachidonic acids: mechanisms and potential therapeutic targets. *Signal Transduct Target Ther* 2021;6:94.
- Wang D, DuBois RN. Eicosanoids and cancer. *Nat Rev Cancer* 2010;10:181–93.
- Murakami M, Taketomi Y, Miki Y, Sato H, Hirabayashi T, Yamamoto K. Recent progress in phospholipase A<sub>2</sub> research: from cells to animals to humans. *Prog Lipid Res* 2011;50:152–92.
- Shimizu R, Engel JD, Yamamoto M. GATA1-related leukaemias. *Nat Rev Cancer* 2008;8:279–87.
- Papaspyropoulos A, Bradley L, Thapa A, Leung CY, Toskas K, Koennig D, et al. RASSF1A uncouples Wnt from Hippo signalling and promotes YAP mediated differentiation via p73. *Nat Commun* 2018;9:424.
- Chang Z, Zhang Y, Liu J, Guan C, Gu X, Yang Z, et al. GATA1 promotes gemcitabine resistance in pancreatic cancer through antiapoptotic pathway. *J Oncol* 2019;2019:9474273.
- Tyrkalska SD, Pérez-Oliva AB, Rodríguez-Ruiz L, Martínez-Morcillo FJ, Alcaraz-Pérez F, Martínez-Navarro FJ, et al. Inflammasome regulates hematopoiesis through cleavage of the master erythroid transcription factor GATA1. *Immunity* 2019;51:50–63.
- Shakib K, Norman JT, Fine LG, Brown LR, Godovac-Zimmermann J. Proteomics profiling of nuclear proteins for kidney fibroblasts suggests hypoxia, meiosis, and cancer may meet in the nucleus. *Proteomics* 2005;5:2819–38.
- Kramer AC, Weber J, Zhang Y, Tolar J, Gibbens YY, Shevik M, et al. TP53 modulates oxidative stress in Gata1(+) erythroid cells. *Stem Cell Reports* 2017;8:360–72.

13. National Research Council (US) Institute for Laboratory Animal Research. Guidance for the description of animal research in scientific publications. Washington, DC: The National Academic Press, 2011.
14. Kashiwagi M, Friess H, Uhl W, Berberat P, Abou-Shady M, Martignoni M, et al. Group II and IV phospholipase A(2) are produced in human pancreatic cancer cells and influence prognosis. *Gut* 1999;45:605–12.
15. Ding XZ, Hennig R, Adrian TE. Lipoxygenase and cyclooxygenase metabolism: new insights in treatment and chemoprevention of pancreatic cancer. *Mol Cancer* 2003;2:10.
16. Eom GH, Nam YS, Oh JG, Choe N, Min HK, Yoo EK, et al. Regulation of acetylation of histone deacetylase 2 by p300/CBP-associated factor/histone deacetylase 5 in the development of cardiac hypertrophy. *Circ Res* 2014;114:1133–43.
17. Kabra DG, Pfuhlmann K, García-Cáceres C, Schriever SC, García VC, Kebede AF, et al. Hypothalamic leptin action is mediated by histone deacetylase 5. *Nat Commun* 2016;7:10782.
18. Xue Y, Lian W, Zhi J, Yang W, Li Q, Guo X, et al. HDAC5-mediated deacetylation and nuclear localisation of SOX9 is critical for tamoxifen resistance in breast cancer. *Br J Cancer* 2019;121:1039–49.
19. Lamonica JM, Vakoc CR, Blobel GA. Acetylation of GATA-1 is required for chromatin occupancy. *Blood* 2006;108:3736–8.
20. Lahm A, Paolini C, Pallaoro M, Nardi MC, Jones P, Neddermann P, et al. Unraveling the hidden catalytic activity of vertebrate class IIa histone deacetylases. *Proc Nat Acad Sci U S A* 2007;104:17335–40.
21. Mihaylova MM, Vasquez DS, Ravnskjaer K, Denechaud PD, Yu RT, Alvarez JG, et al. Class IIa histone deacetylases are hormone-activated regulators of FOXO and mammalian glucose homeostasis. *Cell* 2011;145:607–21.
22. Böttcher JP, Bonavita E, Chakravarty P, Blees H, Cabeza-Cabrero M, Sammiceli S, et al. NK cells stimulate recruitment of cDC1 into the tumor microenvironment promoting cancer immune control. *Cell* 2018;172:1022–37.
23. Basingab FS, Ahmadi M, Morgan DJ. IFN $\gamma$ -dependent interactions between ICAM-1 and LFA-1 counteract prostaglandin E2-mediated inhibition of antitumor CTL responses. *Cancer Immunol Res* 2016;4:400–11.
24. Zelenay S, van der Veen Annemarie G, Jan PB, Kathryn JS, Rogers N, Sophie EA, et al. Cyclooxygenase-dependent tumor growth through evasion of immunity. *Cell* 2015;162:1257–70.
25. Collisson EA, Bailey P, Chang DK, Biankin AV. Molecular subtypes of pancreatic cancer. *Nat Rev Gastroenterol Hepatol* 2019;16:207–20.
26. Hu B, Xu Y, Li YC, Huang JF, Cheng JW, Guo W, et al. CD13 promotes hepatocellular carcinogenesis and sorafenib resistance by activating HDAC5-LSD1-NF- $\kappa$ B oncogenic signaling. *Clin Transl Med* 2020;10:e233.
27. Huang Y, Tan M, Gosink M, Wang KK, Sun Y. Histone deacetylase 5 is not a p53 target gene, but its overexpression inhibits tumor cell growth and induces apoptosis. *Cancer Res* 2002;62:2913–22.
28. Cancer Genome Atlas Research Network. Integrated genomic characterization of pancreatic ductal adenocarcinoma. *Cancer Cell* 2017;32:185–203.
29. ICGC/TCGA Pan-Cancer Analysis of Whole Genomes Consortium. Pan-cancer analysis of whole genomes. *Nature* 2020;578:82–93.
30. Guan Z, Giustetto M, Lomvardas S, Kim JH, Miniaci MC, Schwartz JH, et al. Integration of long-term-memory-related synaptic plasticity involves bidirectional regulation of gene expression and chromatin structure. *Cell* 2002;111:483–93.
31. Yan B, Yang J, Kim MY, Luo H, Cesari N, Yang T, et al. HDAC1 is required for GATA-1 transcription activity, global chromatin occupancy and hematopoiesis. *Nucleic Acids Res* 2021;49:9783–98.
32. Van den broeck A, Gremeaux L, Topal B, Vankelecom H. Human pancreatic adenocarcinoma contains a side population resistant to gemcitabine. *BMC Cancer* 2012;12:354.
33. Burke JE, Dennis EA. Phospholipase A2 structure/function, mechanism, and signaling I. *J Lipid Res* 2009;50:S237–42.
34. Katsumura KR, Bresnick EH, Gata Factor Mechanisms Group. The GATA factor revolution in hematology. *Blood* 2017;129:2092–102.
35. Boyes J, Byfield P, Nakatani Y, Ogryzko V. Regulation of activity of the transcription factor GATA-1 by acetylation. *Nature* 1998;396:594–8.
36. Lamonica JM, Deng W, Kadauke S, Campbell AE, Gamsjaeger R, Wang H, et al. Bromodomain protein Brd3 associates with acetylated GATA1 to promote its chromatin occupancy at erythroid target genes. *Proc Nat Acad Sci U S A* 2011;108:E159–168.